# REPORT DOCUMENTATION PAGE

Public Reporting burden for this collection of information is estimated to average 1 hour per response, including the time for reviewing instructions, searching existing data sources, gathering and maintaining the data needed, and completing and reviewing the collection of information. Send comment regarding this burden estimates or any other aspect of this collection of information, including suggestions for reducing this burden, to Washington Headquarters Services, Directorate for information Operations and Reports, 1215 Jefferson Davis Highway, Suite 1204, Arlington, VA 22202-4302, and to the Office of Management and Budget, Paperwork Reduction Project (0704-0188,) Washington, DC 20503.

| 1. AGENCY USE ONLY ( Leave Blank) | 2. REPORT DATE<br>February 27, 2003 | 3. REPORT TYPE AND DATES COVERED<br>Final Report |
|---|---|---|

| 4. TITLE AND SUBTITLE<br>Computational Tools for Optimized Design of Advanced Traveling Wave Tubes | 5. FUNDING NUMBERS<br>C- F4920-99-C-0064-DEF (STTR Phase II) |
|---|---|
| 6. AUTHOR(S)<br>Carol L. Kory and John H. Booske | |

| 7. PERFORMING ORGANIZATION NAME(S) AND ADDRESS(ES)<br>Analex Corporation<br>21000 Brookpark Road, MS 54-5<br>Cleveland, OH 44135<br><br>University of Wisconsin, Madison<br>1415 Engineering Drive<br>Madison, WI 53706 | 8. PERFORMING ORGANIZATION<br>REPORT NUMBER<br>N/A |
|---|---|

| 9. SPONSORING / MONITORING AGENCY NAME(S) AND ADDRESS(ES)<br>U. S. AF Office of Scientific Research<br>801 N Randolph St<br>Arlington, VA 22203 | 10. SPONSORING / MONITORING<br>AGENCY REPORT NUMBER |
|---|---|

11. SUPPLEMENTARY NOTES
   The views, opinions and/or findings contained in this report are those of the author(s) and should not be construed as an official Department of the Army position, policy or decision, unless so designated by other documentation.

| 12 a. DISTRIBUTION / AVAILABILITY STATEMENT<br><br>Approved for public release; distribution unlimited. | 12 b. DISTRIBUTION CODE |
|---|---|

13. ABSTRACT (Maximum 200 words)
Report developed under STTR contract for topic AF00T002.
Research and development of optimized vacuum electronic sources utilizing advanced computational codes and state-of-the-art micro-fabrication techniques were performed focusing on using micromachining to develop THz regime folded-waveguide traveling-wave tubes (TWTs). Successful development of THz TWTs has enormous potential for low-cost, extremely-high-data-rate (> 10 GB/s) advanced digital communications capabilities, as well as lower cost, higher yield production of millimeter-wave slow-wave amplifiers for air-borne radar and missile seeker technologies.

To address the need for compact THz radiation sources (amplifiers and oscillators), micro-fabricated TWTs were invented under this program and feasibility analyses were completed resulting in representative designs for a 56 mW, 560 GHz recirculated feedback oscillator and a 174 mW, 400 GHz amplifier. The recirculated feedback oscillator concept was successfully demonstrated experimentally at a scaled frequency, and in depth studies have been completed to investigate several parameters including return path attenuation, spectral evolution, small-signal gain, drive characteristics, and phase sensitivity. The first accurate, physics based, particle-in-cell model has been established to represent the recirculated feedback oscillator, and shows good agreement with experimental results. Three complementary microfabrication methods have been explored and compared for eventual commercial feasibility. The methods include xray LIGA, UV LIGA, and DRIE. A fourth method, polymer micromolding, has been identified that shows promise as well, possibly best suited for lower frequencies..

| 14. SUBJECT TERMS<br>STTR Report, vacuum electronics, traveling-wave tube, TWT, oscillator, Terahertz (THz) source, electron device | | 15. NUMBER OF PAGES<br>26 |
|---|---|---|
| | | 16. PRICE CODE |

| 17. SECURITY CLASSIFICATION<br>OR REPORT<br>UNCLASSIFIED | 18. SECURITY CLASSIFICATION<br>ON THIS PAGE<br>UNCLASSIFIED | 19. SECURITY CLASSIFICATION<br>OF ABSTRACT<br>UNCLASSIFIED | 20. LIMITATION OF ABSTRACT<br>UL |
|---|---|---|---|

NSN 7540-01-280-5500

20030312 242

# Computational Tools for Optimized Design of Advanced Traveling Wave Tubes

February 27, 2003

**Contract Number** F4920-99-C-0064-DEF (STTR Phase II)

**TOPIC NUMBER:** AF00T002

**PROPOSAL TITLE:** Computational Tools for Optimized Design of Advanced Traveling Wave Tubes

**FIRM NAME:**
Analex Corporation
Mail Stop: 54-5
NASA, Glenn Research Center
21000 Brookpark Road
Cleveland, Ohio 44135

**PRINCIPAL INVESTIGATOR:** Carol L. Kory

**RESEARCH INSTITUTION:** University of Wisconsin-Madison
**CO-PRINCIPAL INVESTIGATOR:** John Booske

Final Report of Phase II effort covering the period from September 1, 2000 through March 1, 2003

# 1 OBJECTIVES

The objectives of this contract were

- **Thrust Objective**: to develop and research optimized vacuum electronic sources utilizing advanced computational codes and state-of-the-art micro-fabrication techniques. The emphasis of this program was to use micromachining to develop THz regime TWTs with emphasis on folded-waveguide (FWG) TWTs.
- **Research Impact**: very-high-data-rate wireless communications, covert wireless communications (space-space, space-earth, earth-earth), advanced materials spectroscopy sources, high-resolution radar, remote sensing, advanced security scanning, and new THz technology applications.

The terahertz (THz) region of the electromagnetic spectrum ($\sim 300 - 3000$ GHz in frequency or $\sim 0.1 - 1.0$ mm free space wavelength) has enormous potential for high-data-rate communications, advanced electronic materials spectroscopy, space research, medicine, biology, surveillance, and remote sensing. For example, determination of the electrodynamic response of advanced electronic materials, chemicals, and opto-electronic devices in the THz regime is extremely important from a basic science point of view. In this frequency regime, the photon energies span the energies of both quantum correlation gaps in interacting electron systems and conformational resonances in many organic and inorganic molecules. Also, the time scales $t \sim 1/2\pi f$ are of the same order as typical inelastic electron scattering times in many electronic materials and devices. Therefore, with adequately powerful spectroscopic sources covering appreciable bandwidths in the THz regime, one can effectively "undress" a material's basic charge excitations. This allows one to base advanced mm-wave and submm-wave electronic system designs on a fundamental understanding of the intrinsic materials' behaviors at these frequencies, rather than on limited empirical data typically dominated by extrinsic defect or other measurement configuration artifacts. Similarly, clear and precise identification of unique chemical signatures can be obtained from trace amounts of an unknown sample (i.e., remote security monitoring of production of weapons of mass destruction). Using carrier frequencies above 300 GHz, oscillator and amplifier sources with ~10 % fractional bandwidths would enable very high data rate (> 10 GB/s) wireless communications with high security protection. If adequately powerful, compact, and wideband sources were available, this capability could be realized with extremely simple, low-cost amplitude modulation schemes (e.g., simple amplitude modulation and diode receivers).

The critical roadblock to full exploitation of the THz band is lack of coherent radiation sources that are powerful ($0.01 - 10.0$ W CW), efficient ($\geq 1$ %), frequency agile (instantaneous fractional bandwidths > 1 %), reliable, compact, and relatively inexpensive. To minimize the size of the prime power supply, the device voltage should be $\leq 12$ kV in order to utilize compact solid state DC power conditioner technology. Solid state sources satisfy the low voltage requirement, but are many orders of magnitude below the *combined* requirements for power, efficiency, and bandwidth. Typical fast-wave vacuum electronic devices (VEDs) in this regime, such as gyrotrons and free electron lasers, tend to be large, expensive, high voltage and very high power, unsuitable for most of the applications cited above. Figure 1 shows the approximate CW power capabilities in different frequency bands of compact coherent radiation sources that are

currently available based on reports in published literature. It should be noted that both the impatt diodes and the BWO sources have fairly narrow instantaneous bandwidths and very low efficiencies (< 0.01%). Moreover, neither of these high frequency sources provides a high power amplifier capability.
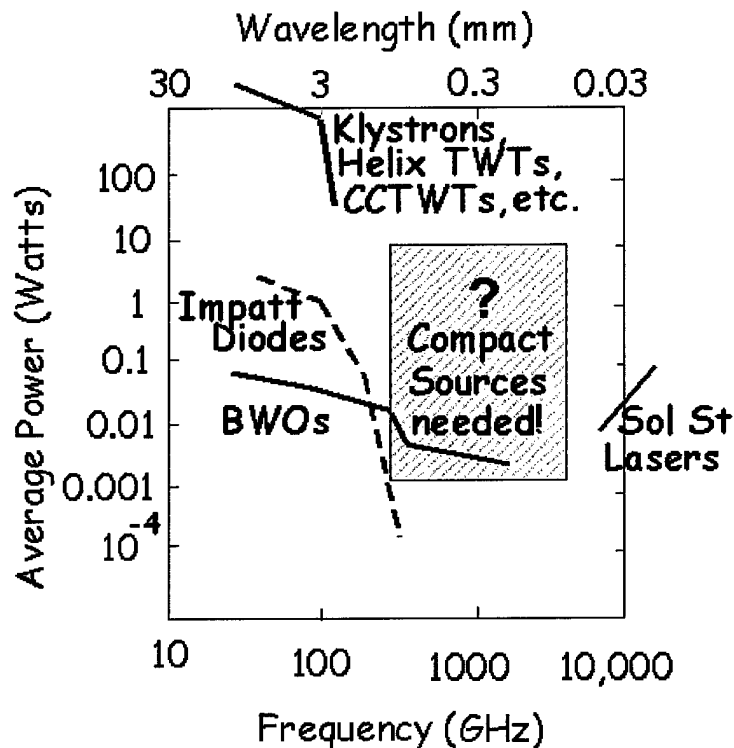


**Figure 1 Compact coherent radiation source capabilities.**

To address the need for compact THz radiation sources (amplifiers and oscillators), we investigated the development of micromachined Vacuum Electronic Devices, or "micro-VEDs" during this Phase II effort. During the past several years, several developments have enabled micron-dimensioned three-dimensional structures (1 – 100 μm). Options include x-ray lithography (LIGA), ultraviolet lithography (using advanced photoresists such as SU-8), micro-electric discharge machining (micro-EDM), and deep reactive ion etching (DRIE) [1, 2, 3, and 4, 5].

Micromachining methods bring a powerful new capability to the VED designer's toolbox. They enable the precision fabrication of microstructures needed for high frequency operation. They introduce mask-based-replication (heretofore the sole domain of solid state microelectronics) that can lead to cost-per-device savings and increased yields. Among other benefits, micromachining can provide superior high frequency wall conductivity as a result of surface smoothness compared with conventional mechanical or EDM approaches.

Micro-VED (μVED) technologies are already being applied to the development of millimeter-wave klystrons at Stanford Linear Accelerator Center [1], THz regime klystrons at the University of Leeds [5] and NASA's Jet Propulsion Laboratory [6], and transit time oscillators at the

University of Michigan [7]. The emphasis of this program has been to investigate micromachining as a means to develop THz regime TWTs with emphasis on folded-waveguide (FWG) TWTs [8].

The FWG-TWT has several features that make it attractive for THz-regime μVED applications: it employs a relatively simple circuit to design and fabricate, it is amenable to micromachining, and it has been demonstrated to be capable of forward-wave amplification with appreciable power and bandwidth [9]. A three-dimensional (3D) view of the FWG slow-wave circuit is shown in Figure 2. We pursued computational and experimental studies of μVED FWG-TWT amplifiers and oscillators to establish their feasibility for sources in the $0.2 - 1.0$ THz frequency regime.
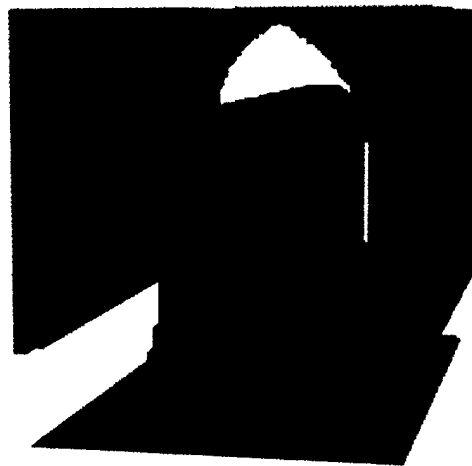


**Figure 2 Three-dimensional cutaway view of one bend in a simulated folded waveguide circuit using MAFIA.**

The task descriptions for the Phase II effort were as follows:
**TASK 1. Obtain optimized vacuum device designs.**
Using advanced electromagnetic codes and the vast experience of the proposal team, several vacuum electronic devices were investigated by designing several devices with similar operating parameters and comparing their performance. Computational analyses included cold-test and large signal analyses. An optimum device design was determined from the results of these investigations.

**TASK 2. Fabrication**
University of Wisconsin investigated methods to fabricate the devices designed under Task 1. Prototype circuits were fabricated in UW shops, outside shops, or a combination of both. UW machine shops, researchers, and research staff have prior experience in similar microwave circuit fabrication tasks, and they drew upon this experience.

**TASK 3. Experimental validation**
Scaled laboratory experiments were conducted to confirm the computational design predictions.

**TASK 4. Documentation**

-4-

All reporting requirements as stated in the STTR Phase II contract have been met, with the submission of this final report. In addition, progress has been described at international IEEE sponsored conferences as well as in IEEE sponsored journals.

Table 1 shows a detailed chart that identifies critical dates, tasks, and deliverables associated with the work performed.

### Table 1 Critical dates, tasks and deliverables

| Quarter | Task | Deliverables |
|---------|------|--------------|
| **YEAR 1** | | |
| 1-4 | Investigate several vacuum device designs | Computational analyses |
| 1-4 | Investigate fabrication techniques for low loss, high performance devices | Fabricated prototype circuits and material characterization results |
| 1-4 | Prepare experimental test stand for device characterization | Experimental test stand for device characterization |
| **YEAR 2** | | |
| 1-2 | Complete optimized device design based on comparisons completed in year 1 | Complete specification of optimized device geometry and operating parameters |
| 1-2 | Establish fabrication procedure for optimized device | Established fabrication procedure for optimized design |
| 2-3 | Fabricate scale model of optimized design | Fabricated scale model |
| 3-4 | Experimental characterization of device. | Experimental device data |

## 2 Status of Effort

We have introduced planar traveling wave tubes in designs suitable for batch fabrication and operation at frequencies approaching the terahertz regime. Simulations with a variety of specialized tools indicate intrinsic efficiencies of 1% for ~ 600 GHz operation under realistic conditions, resulting in compact and ultimately inexpensive sources of ~ 56 mW power at these frequencies.

Optimized designs for representative folded waveguide amplifiers and oscillators have been completed using a suite of high-level computational tools. Several fabricated prototype circuits have been completed based on these designs. Various microfabrication approaches have been explored and contrasted for commercial feasibility. Experimental testing of one concept for a TWT oscillator using a scaled experiment at 50 GHz has shown good correlation between simulated predictions and laboratory measurements.

# 3 Accomplishments/New

- Invented and completed feasibility analyses for micro-fabricated TWTs that will enable low-cost, extremely-high-data-rate (> 10 GB/s) advanced digital communications capabilities using THz frequencies, as well as lower cost, higher yield production of millimeter-wave slow-wave amplifiers for air-borne radar and missile seeker technologies.
- Successfully demonstrated the recirculated feedback oscillator concept experimentally at a scaled frequency. In depth studies have been completed to investigate several parameters including:
  - return path attenuation
  - spectral evolution
  - small-signal gain
  - drive characteristics
  - phase sensitivity
- The first accurate, physics based, particle-in-cell model has been established to represent the recirculated feedback oscillator. The model shows good agreement with experimental results.
- Three complementary microfabrication methods have been explored and compared for eventual commercial feasibility. The methods include xray LIGA, UV LIGA, and DRIE. A fourth method, polymer micromolding, has been identified that shows promise as well, possibly best suited for lower frequencies.

As reported in the first year's annual report, several folded waveguide (FWG) slow-wave circuits were designed and analyzed using computational models. The most promising slow-wave circuit for THz applications in terms of the feasibility of accurate fabrication and performance is the folded waveguide circuit as sketched in Figure 3.
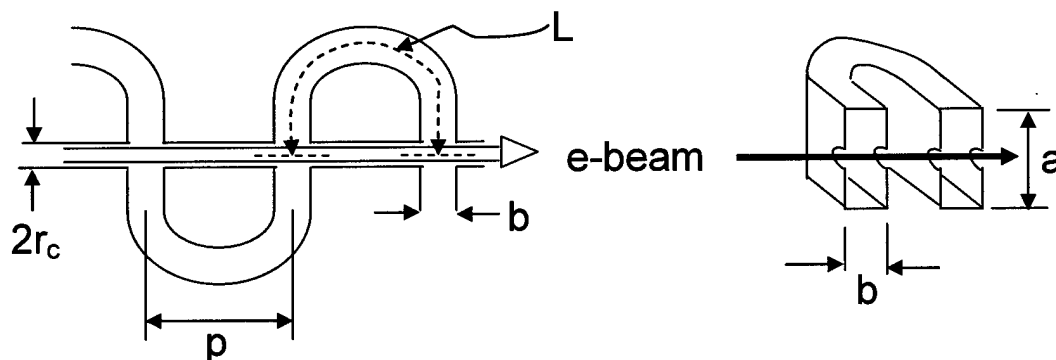


**Figure 3 Folded waveguide circuit sketch. Indicated are the transverse dimensions, *a* and *b* of the rectangular guide, and the beam hole radius, $r_c$.**

Designing FWG-TWTs to meet gain, bandwidth, power, and operating frequency band specifications is nontrivial due to the dispersive properties of the circuit, the effect of beam space charge on the gain and operating bandwidth, and the effect of ohmic wall losses, which are significant at THz regime frequencies. To realize an efficient and reliable design approach, we

coordinated the use of several recently developed computational tools: MAFIA, HFSS, TWA3, and CHRISTINE1D. Slow-wave circuit cold-test data is obtained using the 3D electromagnetic codes MAFIA [10] and HFSS [11], and used as input into the TWT interaction codes, TWA3 [12] and CHRISTINE1D [13] to determine gain and power transfer characteristics. In addition, the time-domain, particle-in-cell (PIC) simulation feature of MAFIA allowed us to conduct interaction simulations, as well as qualitative examinations of transient startup phenomena in THz regime oscillators that utilize a FWG-TWT as the active gain part of the device.

Using these computational models, we developed realistically achievable designs for a 560 GHz oscillator and a 400 GHz amplifier as described below.

### 3.1 56 mW, 560 GHz, FWG-TWT Oscillator

An optimized design was determined for the FWG-TWT slow-wave circuit for operation at ~ 560 GHz. The dimensions and representative geometry are shown in Table 2. The dispersion diagram is shown in Figure 4 and the on-axis interaction impedance and attenuation (wall conductivity was assumed to be about $4 \times 10^7$ S/m) are shown in Figure 5.

**Table 2 Dimensions of 560 GHz folded waveguide slow-wave circuit ($\mu$m)**

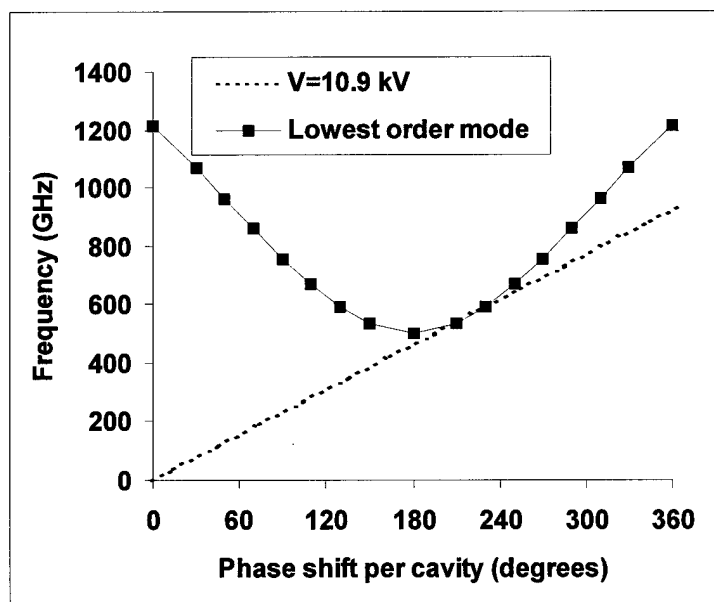| | |
|---|---|
| b | 43 |
| a | 300 |
| $R_{avg}$ | 33 |
| l | 32 |
| $r_c$ | 10 |
| p | 66 |



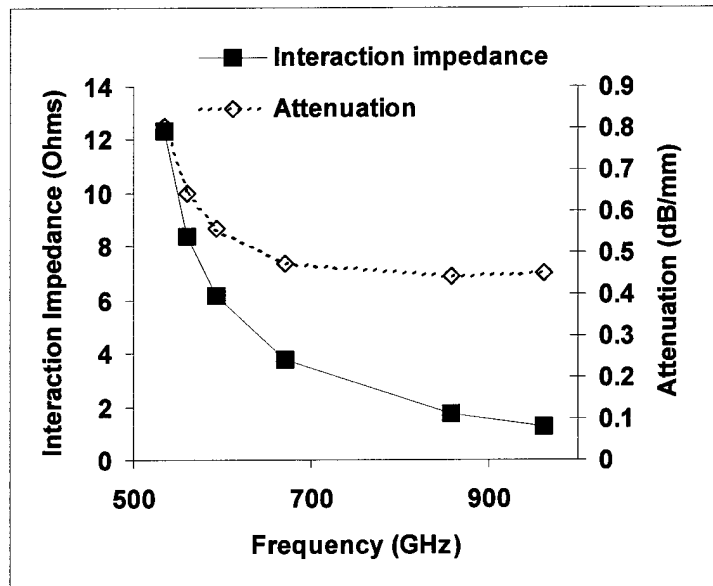**Figure 4 Simulated dispersion for FWG circuit with 10.9 kV beamline.**

**Figure 5 Simulated interaction impedance and attenuation**

Shown in Figure 6 are the results of a calculation of the small-signal gain of a short, 6.6 mm long section of the circuit, assuming a 10.9 kV, 0.5 mA electron beam. The gain was calculated with several different computational models and compared. The MAFIA simulations were done for a lossless circuit only, but the agreement with the parametric code TWA3 is excellent. Furthermore, both TWA3 and CHRISTINE1D agree in predicting approximately 10 dB gain between 520 and 580 GHz (a 10% fractional instantaneous bandwidth) when wall losses are included (assumes an effective wall conductivity of $\sigma \sim 4 \times 10^7$ S/m).
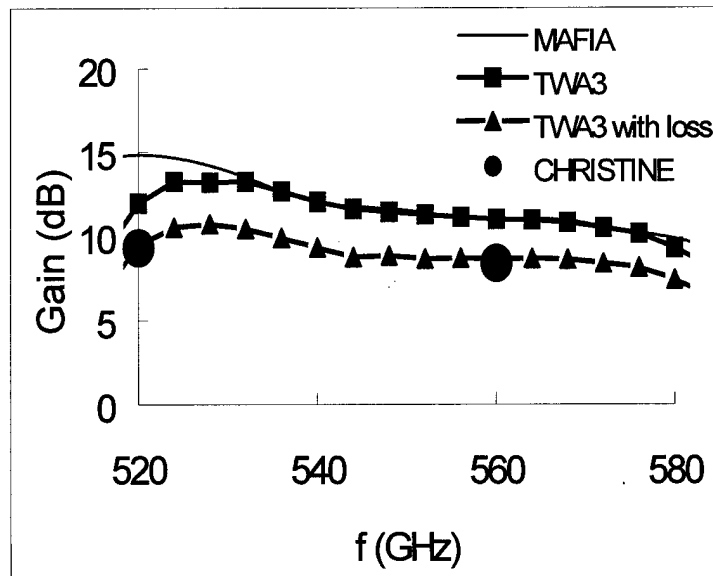


**Figure 6 Small signal single pass gain for a 6.6 mm long FWG-TWT designed to operate at ~ 560 GHz. The simulation assumes a 10.9 kV, 0.5 mA electron beam.**

To investigate achievable levels of output power, large-signal simulations were also completed. For this example, a 2.5 cm long circuit was predicted using CHRISTINE1D to produce ~ 23 dB of gain at ~ 560 GHz. Saturated output power was predicted to be ~ 73 mW, as shown in Figure 7.
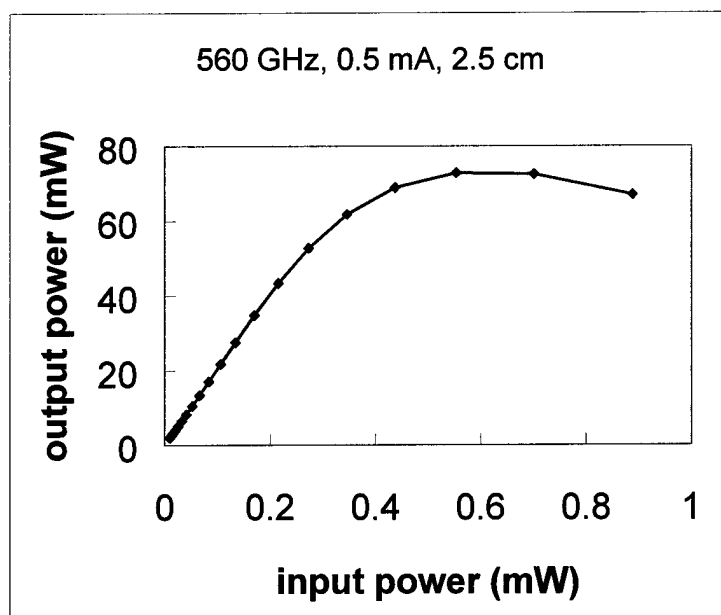


**Figure 7 Drive curve predicted by CHRISTINE1D for 10.9 kV, 0.5 mA, 2.5 cm, 560 GHz FWG-TWT amplifier. Saturated power is about 73 mW.**

We considered several options for feedback to examine whether this circuit could be converted to a ~ 600 GHz oscillator. Reflecting the forward power back along the FWG circuit (a "Fabry-Perot" approach) is impractical due to the high ohmic losses suffered by the reflected wave at THz frequencies. However, recirculating a fraction of the forward wave back to the input of the circuit through a separate, straight, return leg is a viable option (Figure 8). Additional reductions of loss on the recirculated power are possible by up-tapering the small lateral dimension of the rectangular waveguide, as suggested in Figure 8. Analytic estimates of the losses experienced in the recirculation leg combined with the predicted forward gain lead to an approximate self-consistent prediction of steady state radiated power of ~ 56 mW at 560 GHz for a 2.5 cm long circuit and a 10.9 kV, 0.5 mA electron beam. This represents an intrinsic efficiency of 1%, which is substantially higher than either solid state or BWO sources at this frequency. Figure 1 shows that a 56 mW, 560 GHz oscillator is well within the indicated region where compact, efficient sources are needed. It should be noted that increased device efficiency and decreased waste heat dissipation at the beam collector can be expected from the use of a depressed voltage collector.
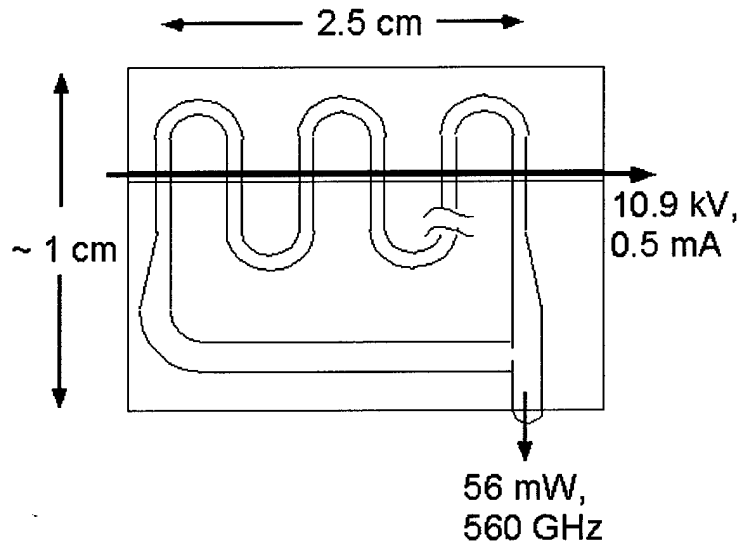
**Figure 8  Schematic illustration of 560 GHz, 56 mW folded waveguide TWT oscillator.**

### 3.1.1  Recirculated Feedback Oscillator Particle-in-Cell (PIC) Simulations

Although the recirculated feedback oscillator approach is promising, there was no computational model to predict the device behavior.  Therefore, the 3D PIC solver of MAFIA was used to investigate spontaneous RF excitation of the recirculated feedback oscillator configuration.  A lossless structure was assumed and the geometry simplified slightly as shown in Figure 9 to reduce computational time.  The total FWG length was determined by using TWA3 [12] to obtain the length that would achieve about a 10 dB gain if the circuit were in the conventional TWT configuration (~ 1 cm).  In fact, it was determined that the selected length corresponded to a forward gain of approximately 9.75 dB.  The waveguide return path is not up-tapered (as it would be for loss reduction) since wall losses are neglected in the simulation.  The strength of the feedback signal was controlled in the simulation by filling a portion of the recirculation leg with a lossy dielectric material.  The amount of lossy material was varied to achieve four cases of attenuation in the return path: (a) 0 dB, (b) –8.75 dB, (c) –9.75 dB, and (d) –10.75 dB.  The other operating and simulation parameters are summarized in Table 3 and Table 4, respectively.

The computation times were very large, and hence it was only practical to simulate the initial onset of oscillation.  In particular, the length of the simulation time was restricted to the equivalent of approximately nine full round-trip transits of the electromagnetic energy.

The wave's electric field was monitored at point "P1" in the recirculation leg, as indicated in Fig. 9 below.  Figure 10 shows a typical evolution of the transverse wave electric field component with time.  It is obvious that this system operates as a spontaneous oscillator.

Discrete Fourier transforms (DFTs) were computed to observe how the wave's frequency evolved with time.  Figure 11(a) illustrates an overdriven case of large feedback with 0 dB return loss.  The spectrum does not lock onto any single frequency, and a broad, multifrequency oscillation spectrum over the 528 – 580 GHz regime is observed.  When the return path loss is increase to approximately –8.75 dB, the oscillator appears to self-select two preferred frequency

-10-

states around 520 and 580 GHz, as seen in Fig. 11(b). When the loss is further increase to –9.75 dB, oscillation in a single frequency state at 580 GHz is observed, as shown in Fig. 11(c). Finally, when the loss is increased to 10.75 dB, there is no spontaneous signal growth as the loss in the return path exceeds the forward gain.
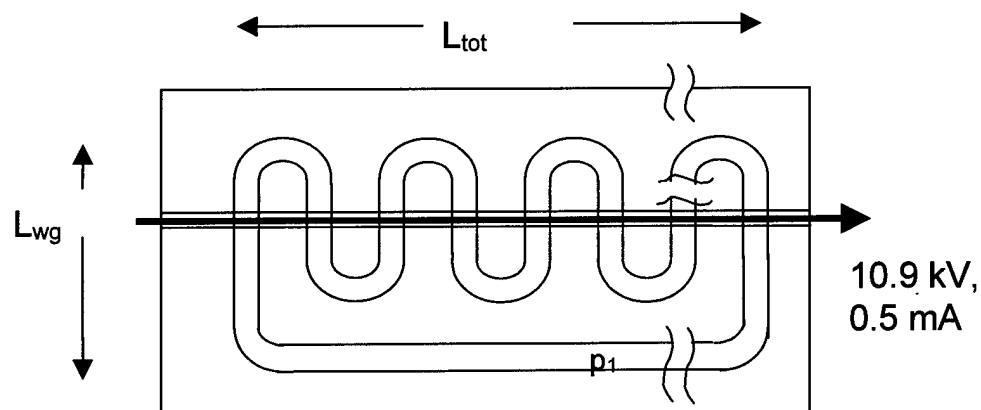


**Figure 9 Schematic illustration of simplified MAFIA 560 GHz folded waveguide TWT oscillator**

**Table 3 Operating parameters of folded waveguide oscillator**

| | |
|---|---|
| Beam current (mA) | 0.5 |
| Beam voltage (kV) | 10.9 |
| Axial magnetic flux density (T) | 0.67 |
| Beam radius /beam tunnel radius ($r_b/r_c$) | 0.7 |

**Table 4 MAFIA simulated folded waveguide oscillator parameters**

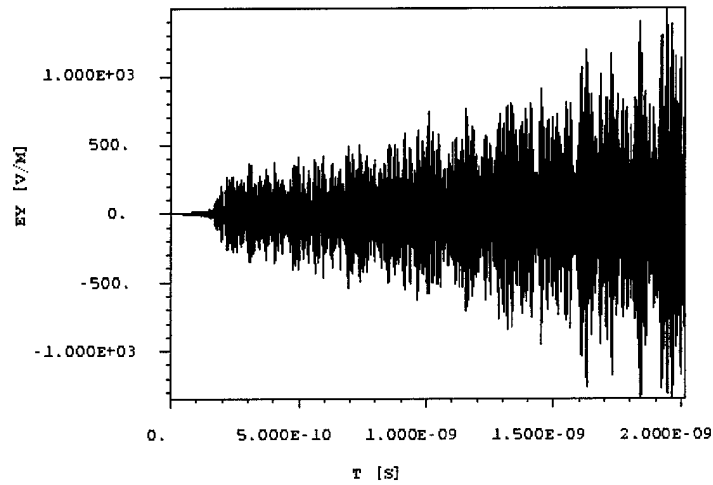| | |
|---|---|
| $L_{tot}$ (cm) | 1.01 |
| $L_{wg}$ (cm) | 0.055 |
| Number of folded waveguide cavities | 154 |
| Approximate time to propagate one complete path, $t_p$ (ns) | 0.19 |

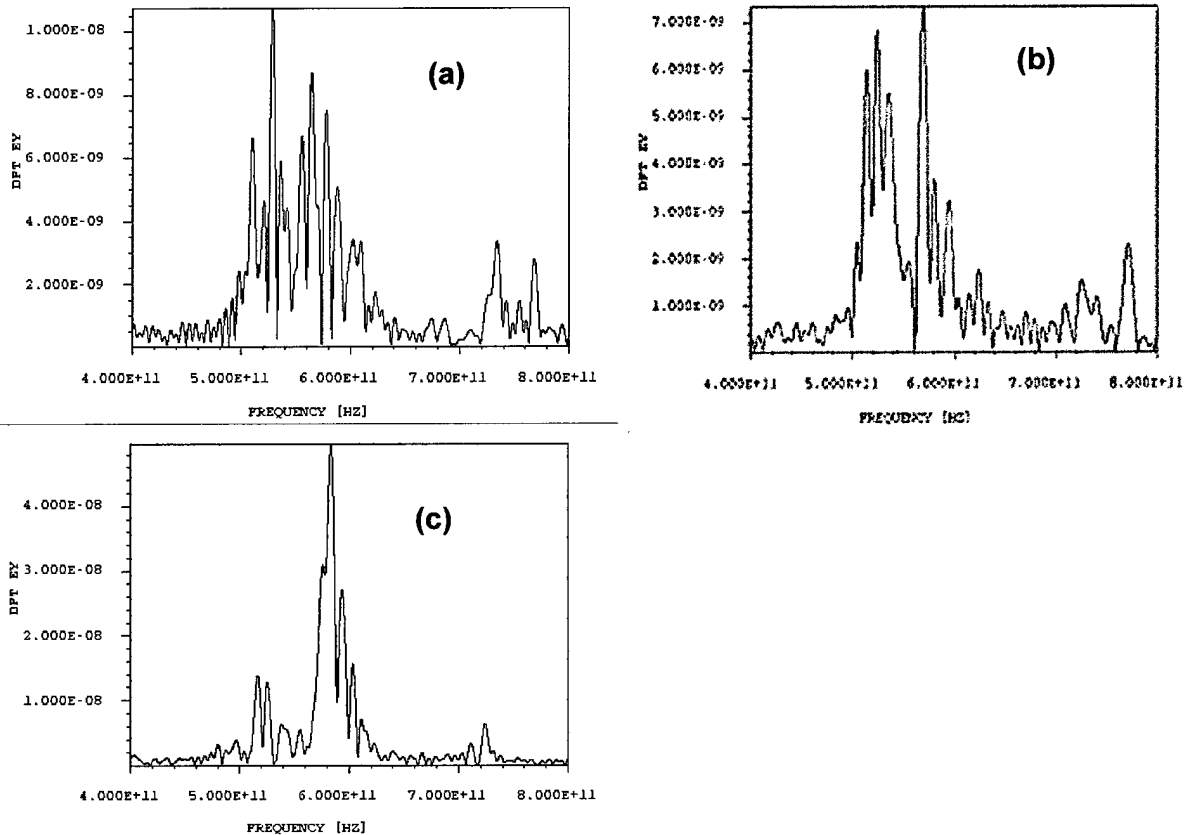**Figure 10 Simulated y-component of electric field at position p1 of Figure 9.**



**Figure 11 Simulations showing frequency selection for the 560 GHz oscillator. (a) 0 dB loss. Overdriven feedback having multi frequency oscillation states. (b) - 8.75 dB loss. Intermediate feedback, showing two preferred frequency states and (c) - 9.75 dB loss. Critical feedback showing approach to a single frequency state.**

When the (time-integrated) DFT spectrum showed multiple frequencies, it was of interest to know whether this represented unstable hopping between the frequencies or simultaneous generation of multiple frequencies. Discrete Fourier Transforms do not provide the answer to this question, particularly when the spectral evolution occurs on a relatively rapid timescale. As the time window is narrowed, for example, one loses resolution and the information becomes distorted. Joint time-frequency analysis (TFA) eliminates the uncertainty of the windowed DFT. In collaboration with researchers from the University of Michigan, the simulation data were analyzed with TFA. Figures 12(a) and 12(b) show the results for the intermediate and critical feedback cases of –8.75 dB and –9.75 dB return loss, respectively. In Fig. 12(a), the instantaneous spectrum is observed to be rapidly hopping between two preferred frequency states at 520 and 580 GHz. For critical feedback at –9.75 dB return loss, the frequency hopping is not observed. Instead, the oscillator is observed to have settled into one "preferred" state at 580 GHz.
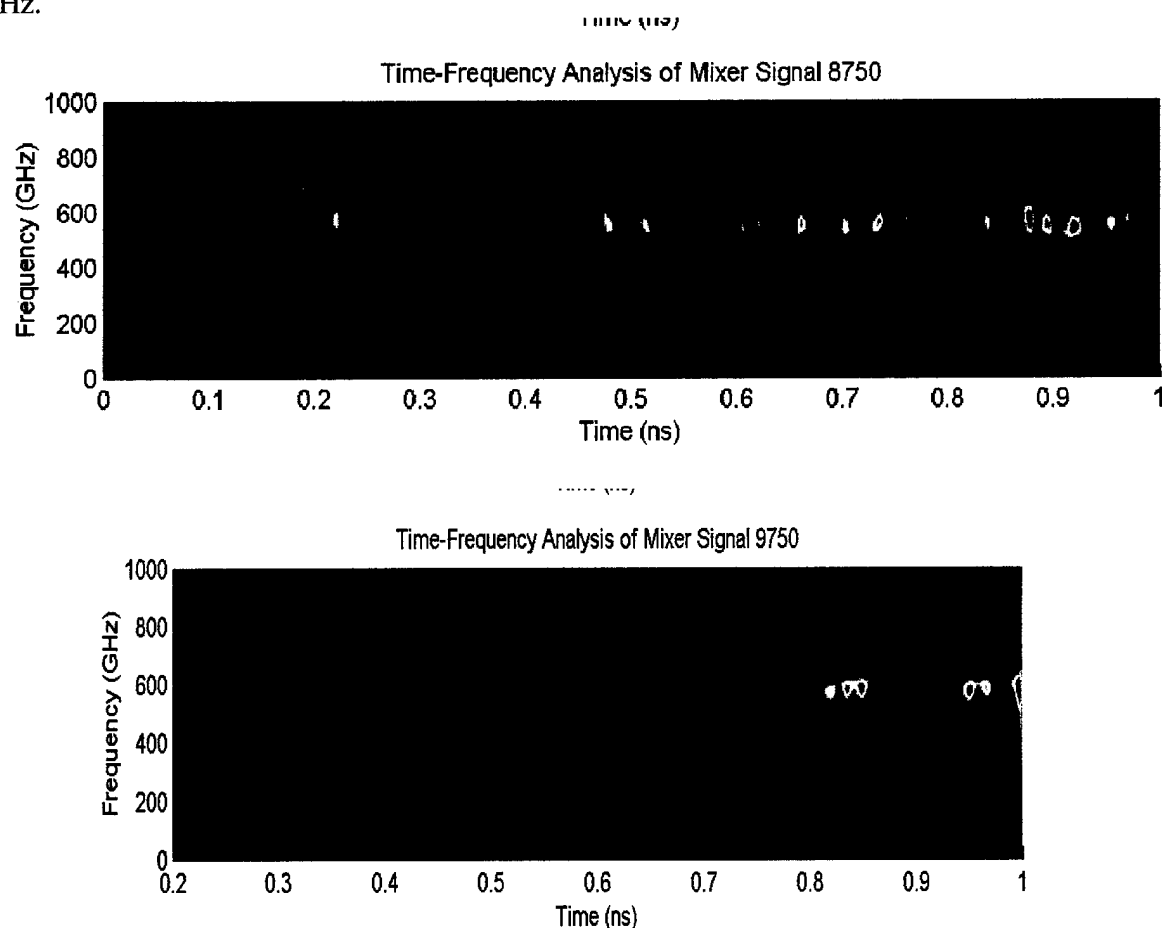




**Figure 12 Time frequency analysis. (a) Intermediate feedback (-8.75 dB return loss) (b) Critical feedback (-9.75 dB return loss).**

### 3.1.2 Scaled Experiments with TWT Oscillator

The basic operating principles of a TWT oscillator with recirculated feedback are not known to have been previously reported. There are a number of important fundamental issues to

investigate concerning oscillation thresholds and oscillation states. Since FWG-TWTs can have up to a 30% fractional bandwidth, it is important to determine what frequency (or frequencies) will be self-selected in the saturated oscillation state. The fraction of output power that is fed back to the input is expected to affect whether the device operates below start oscillation, at critical oscillation equilibrium, or in an overdriven state.

To investigate the physics of the oscillator, a scaled experiment at 50 GHz was carried out. Figure 13 shows a schematic of the experimental assembly. The amplifier has been converted into an oscillator by using an external feedback loop which consists of waveguide components, a variable attenuator to vary the level of output power fed back to the input, and a T-coupler for coupling a fraction of the output power into a spectrum analyzer for measurement purposes.

By varying the attenuation in the feedback leg using the variable attenuator, we observed the self-selected oscillation frequencies at different feedback power levels. The total attenuation in the feedback leg could be varied between –3 and –30 dB over the 40 to 50 GHz range. At full attenuation, no oscillations are observed at any frequency (Figure 14(a)). The critical feedback threshold appears at ~ -26 dB where stable single frequency oscillations at 43.4 GHz were observed (Figure 14(b)). The single frequency oscillations persist until –15.1 dB (Figure 14(c)), where a second frequency at 42.5 GHz appears. At –8.25 dB feedback, the frequency at 43.4 GHz has disappeared while a new oscillation at 43.6 GHz appears along with the one at 42.5 GHz. At –7.0 dB, frequencies are 42.7 GHz, 43.1 GHz and 43.6 GHz appear simultaneously (Figure 14(e)). Finally, at even lower levels of attenuation, no clear tendency is observed, and the spectrum consists of many frequency components in the range 40-50 GHz, as indicated in Figure 14(f). All of the observations in Figure 14 are consistent with the predictions from the MAFIA simulations.

To examine the stability of the oscillations to the feedback signal's phase, a Q-band (33-50 GHz) phase shifter was placed in the feedback circuit. The phase of the feedback signal was varied from 0 – 360 degrees with respect to the input signal and changes in the oscillation spectrum were recorded. Figure 15 shows the sensitivity of the oscillations to changes in feedback phase. Measurements were made for cases where single frequency oscillations were observed, close to critical feedback. It is seen that the oscillations show some sensitivity to changes in feedback phase, but this sensitivity is rather modest. In fact, the frequency remains stable against changes in feedback phase between 60-220 degrees, although for some values of phase the frequency can change by up to 1 GHz rather abruptly. The fact that the frequency was not a sensitive function of the feedback phase is consistent with the feedback delay time (~ 1 ns) being much longer than the period of oscillation (0.02 ns at 50 GHz). The phase sensitivity and stability is a subject of continuing investigation.
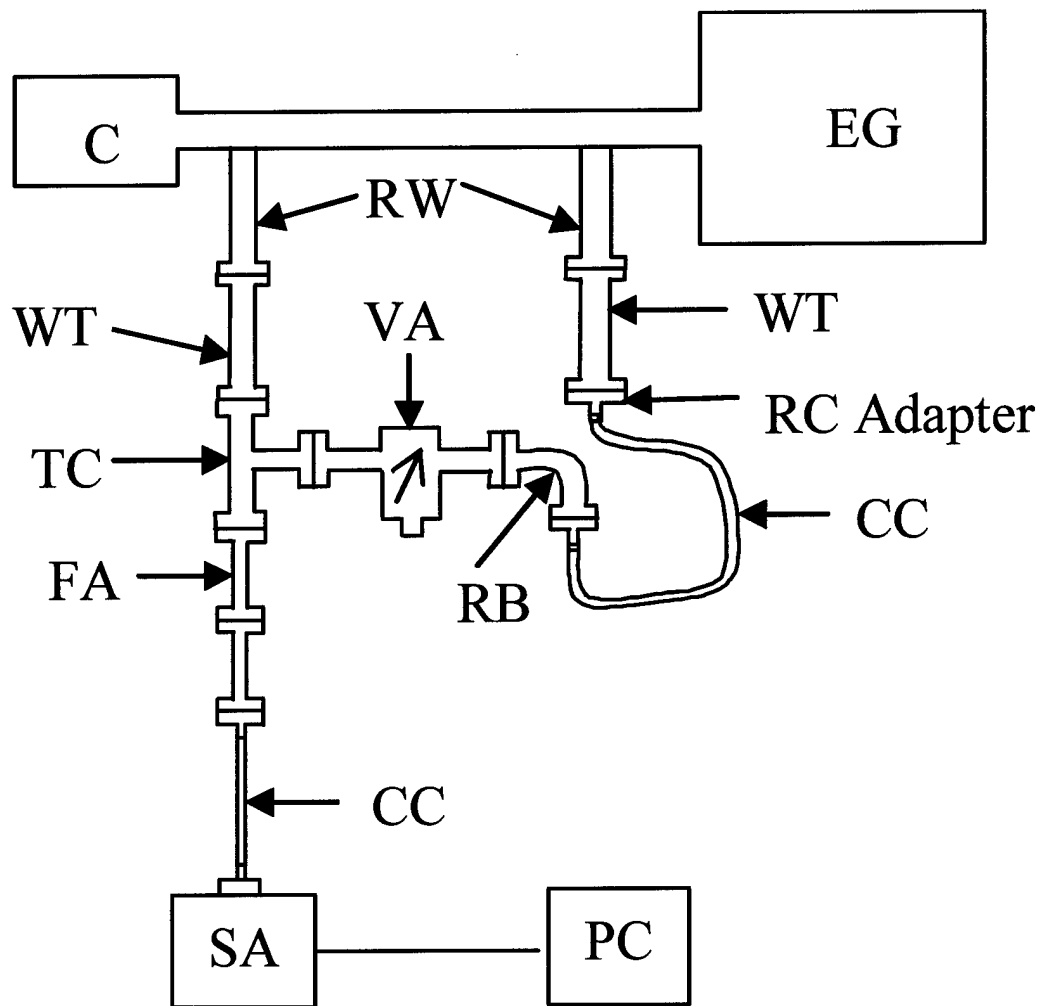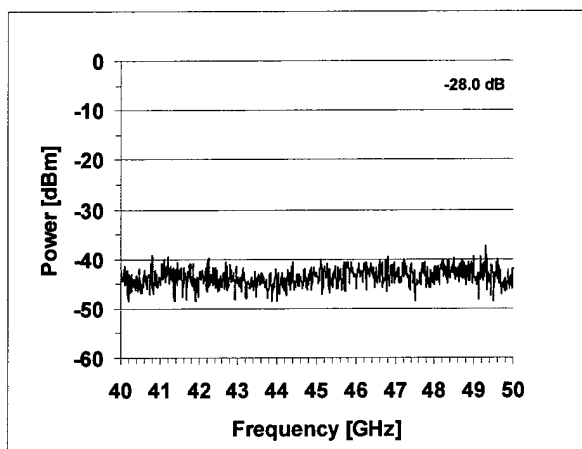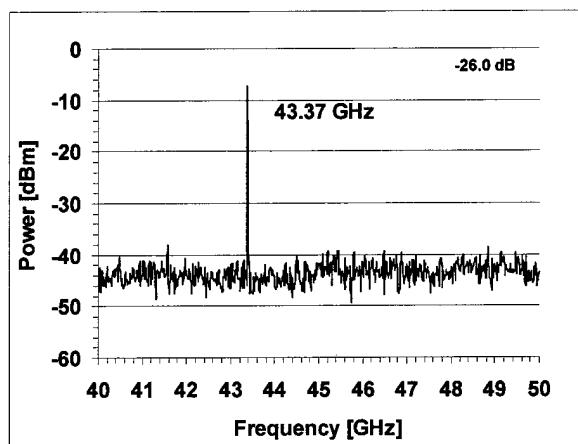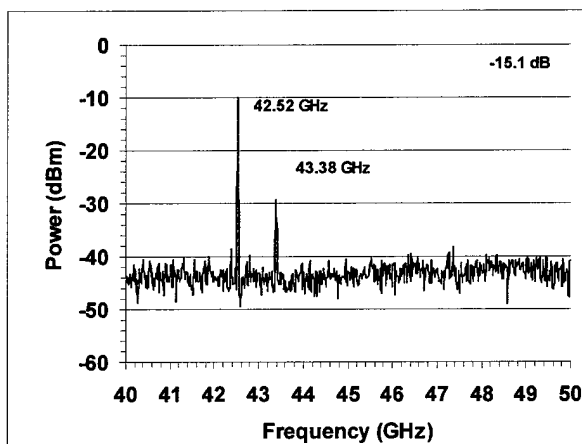
**Figure 13 A schematic of the experimental system for the 50 GHz FWG-TWT Oscillator. C: Collector, E: Electron Gun, RW: Rectangular Waveguide (WR19), WT: Waveguide Transition (WR19 to WR22), RC: Rectangular to Coaxial Adapter, CC: Coaxial Cable, RB: Rectangular Bend, VA: Variable Attenuator, TC: T-Coupler, FA: Fixed Waveguide Attenuator, SA: Spectrum Analyzer, PC: Computer.**
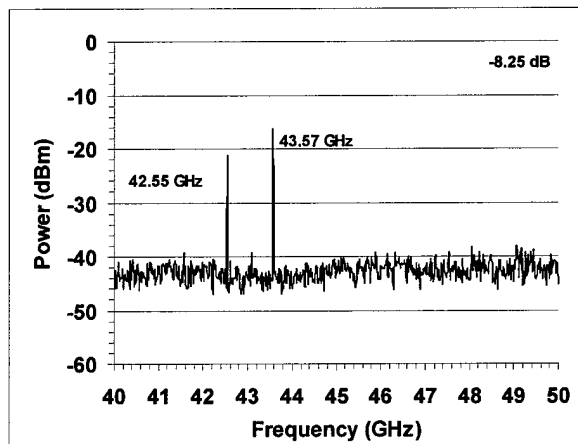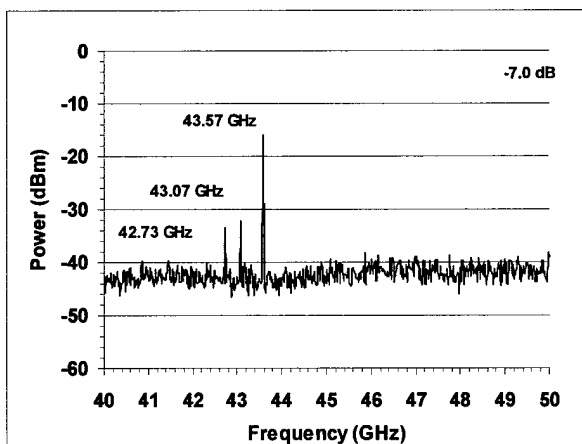
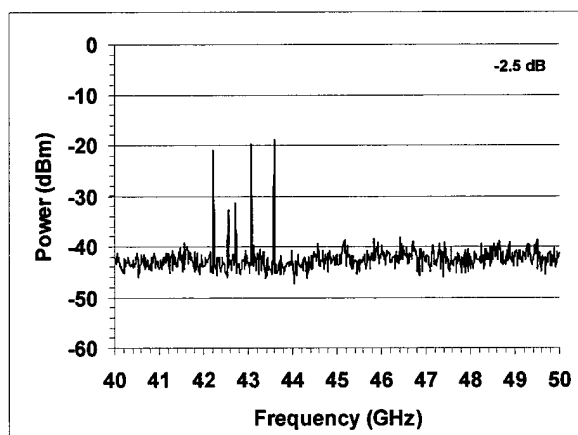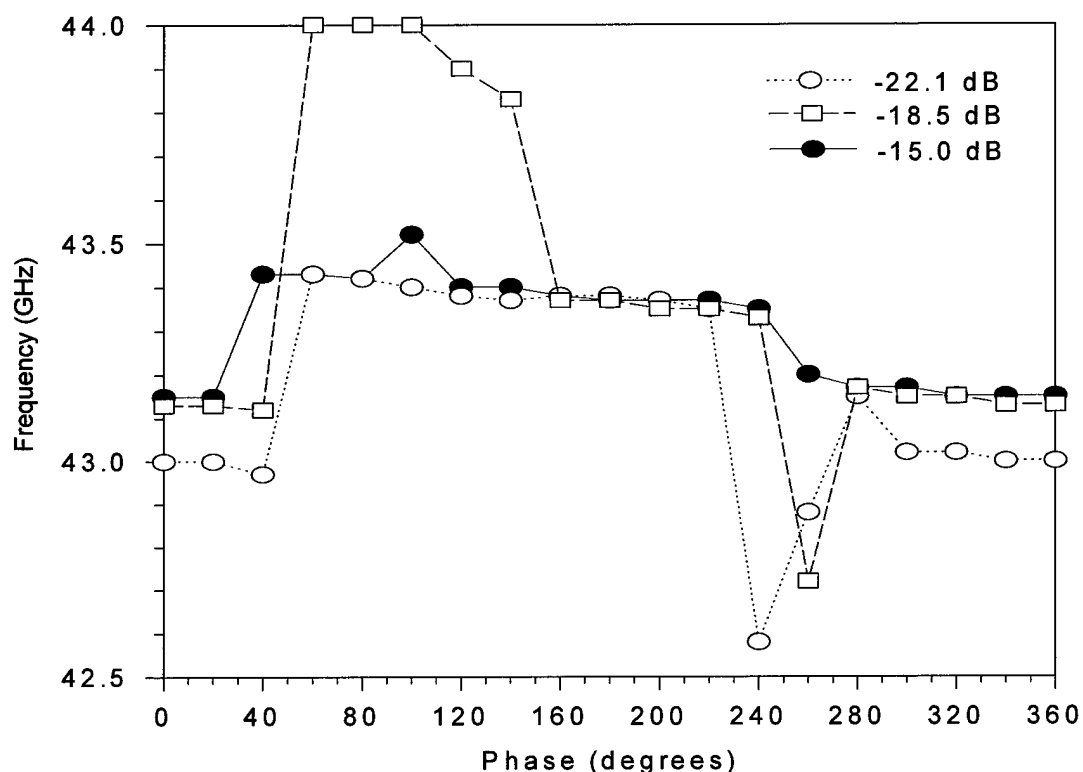**Figure 14  Spectral evolution with feedback attenuation**

**Figure 15 Phase sensitivity of the generated oscillations.**

## 3.2 174 mW, 400 GHz, FWG-TWT Amplifier

The suite of computational codes were also used to design a 174 mW, 400 GHz FWG-TWT amplifier assuming a 12 kV, 3 mA electron beam. Figure 15 illustrates the simulated small-signal gain for a 370-420 GHz, 10 dB gain, self-consistent, FWG-TWT amplifier design that we will use as the basis for proof-of-concept experiments. The gain calculations including loss in Fig. 16 assume conservative effective wall conductivity for copper of $3x10^7$ S/m. Computations show a saturated output power of 174 mW for a three cm long circuit.
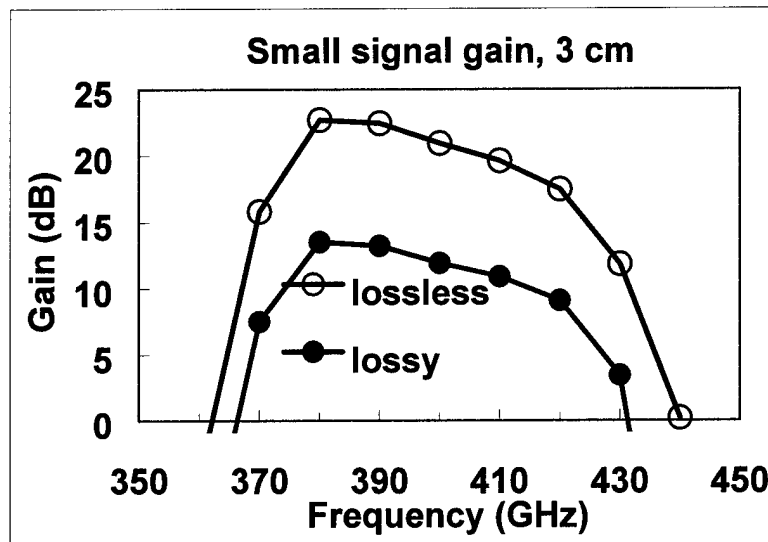
**Figure 16 Small signal gain for a three cm long FWG-TWT amplifier designed to operate at 400 GHz.**

### 3.3 FWG Circuit Fabrication

As part of this research project, we have investigated four complementary methods for batch fabrication of miniature folded waveguide TWT circuits: X-ray LIGA, UV LIGA, deep reactive ion etching (DRIE), and polymer micromolding. Collaborating with Argonne National Laboratory (ANL), we have explored the use of LIGA. In its most familiar form, LIGA uses xrays from a synchrotron, a gold, patterned xray mask, and polymethyl-methacrolate (PMMA, or "Plexiglas") photoresist to generate a "3D negative" mold of the desired structure. The PMMA mold is subsequently filled with metal by electroplating to produce the desired structure. In our case, those structures are copper folded-waveguides (or waveguide halves—two such halves bonded together form a complete waveguide circuit).

The design and fabrication on an optical lithography mask for 400 GHz test structures was completed. The layout contained several straight waveguide circuits, as well as FWG-TWT oscillator circuits similar to that depicted in Figure 8. The optical masks were used to make xray lithography masks, which, in turn, were used for deep xray exposure of PMMA xray photoresist. Figure 17 shows the 400 GHz FWGTWT circuit optical photomask for LIGA and its exploded view.

Xray exposures were conducted by University of Wisconsin personnel in collaboration with ANL collaborators and the developed PMMA molds have been successfully electroplated. A final evaluation of the structures has not been completed. The copper-in-PMMA samples need to be uniformly polished to the specified height followed by additional copper electroplating. After these two steps, the PMMA can be removed and the samples can be inspected for dimensional accuracy, microstructure (small grain size) and surface finish. Figure 18 below shows a collage of images associated with the results to date.
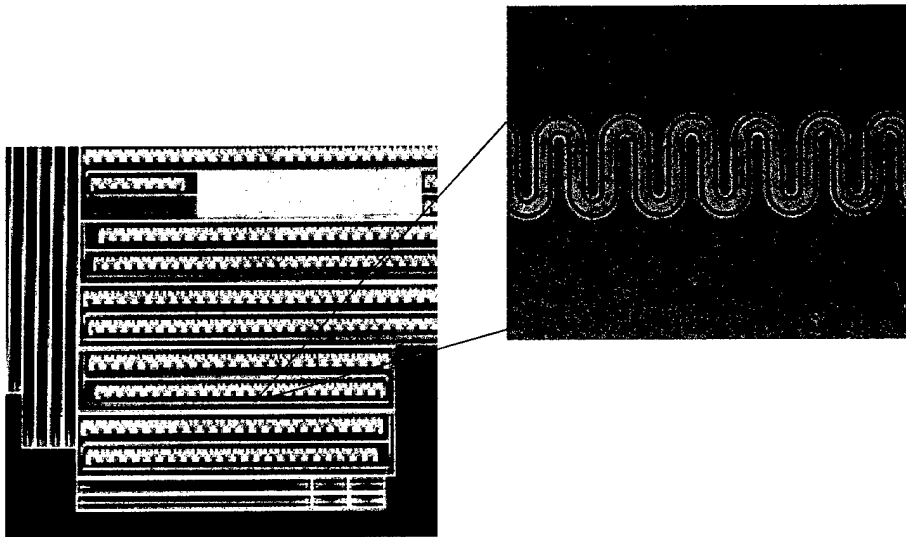
**Figure 17 First results of a 400 GHz FWGTWT circuit optical photomask for LIGA. The inset shows the exploded view of a serpentine waveguide circuit.**

One anticipated constraint of X-ray-based LIGA is the requirement for access to an intense source of high-energy X-ray radiation. In the U.S., there are only three such facilities in existence (Argonne, Brookhaven, and Berkeley) and only one commercial foundry to provide exposure capabilities on an out-source basis. In view of this potential barrier to commercialization of LIGA-fabricated structures, a second exploratory investigation has also been initiated. This alternative approach uses ultraviolet (UV) lamps to expose a UV-sensitive photoresist, SU-8. This procedure is even less mature than X-ray photolithography using PMMA. However, if it can be successfully and fully developed, it offers a very important advancement. In particular, the required UV exposure facilities are relatively common (compared to X-ray generating synchrotrons). They can be found in most microelectronics developing laboratories and foundries, and are quite affordable to manufacturing organizations that wish to develop an in-house LIGA capability. Again, however, experience with SU-8 exposure and development is relatively new and additional process research and development is needed to establish reliability and optimization. Nevertheless, some preliminary efforts have been completed using the same optical mask designed for the 400 GHz folded waveguide circuits. So far, after several attempts, SU-8 molds were successfully produced after UV exposure and subsequent chemical development. Figure 19 shows a scanning electron micrograph of one such mold, having been fractured at the end to allow for a three-dimensional perspective view. The next step for fabrication would be to take a complete such mold, and copper electroplate, polish, electroplate, and remove the PMMA, just like with X-ray LIGA.
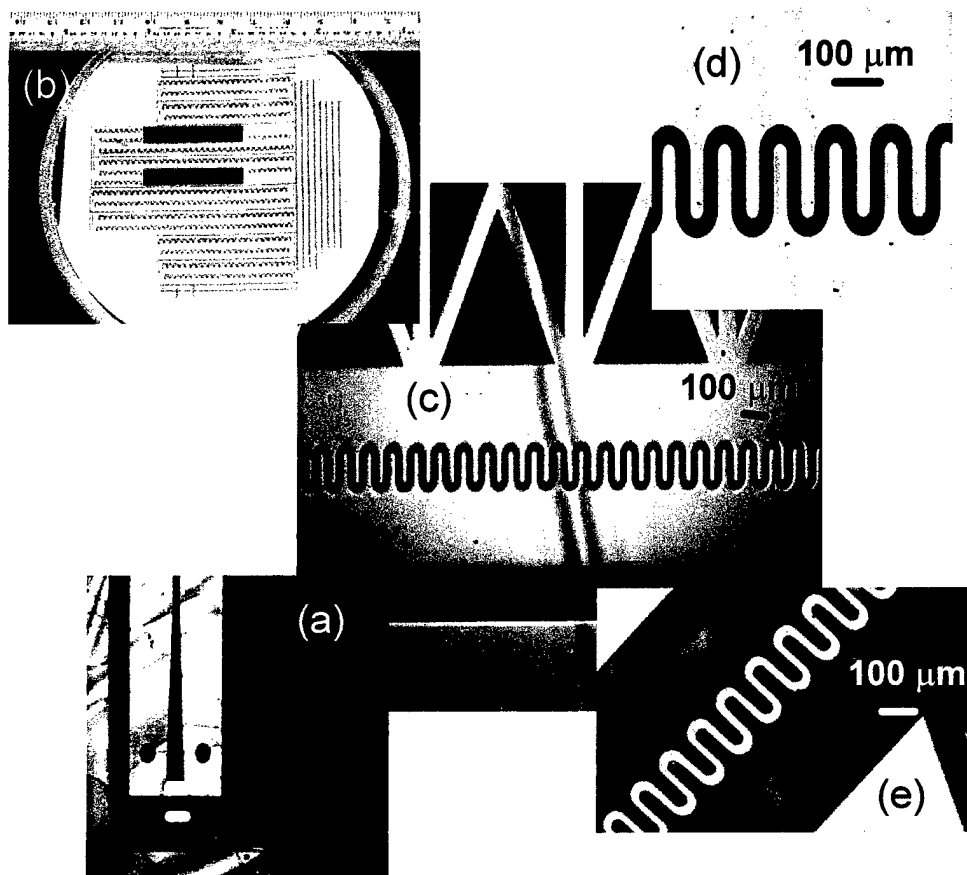
**Figure 18 Microfabrication of 400 GHz folded waveguide TWT circuits using xray lithography and LIGA. The process requires producing a gold mask for xray lithography, exposure of PMMA with xrays to produce a polymer "negative" of the desired circuit, and copper electroplating around the PMMA structure. Clockwise, starting in the lower left corner: (a) xray mask for flared waveguide input/output couplers—copy on left still has PMMA resist on top, dark copy on the right has had PMMA resist removed; (b) gold xray mask on a 10 cm diameter wafer with multiple circuits ready for xray exposure; (c) closeup view of one folded waveguide circuit on the gold xray mask—the truss-like features are for mechanical support; (d) closeup view of serpentine shown in "c"; (e) near-final stage of folded waveguide circuit fabrication: xray photoresist (PMMA) has been exposed and etched and first copper electroplating step has been completed.**
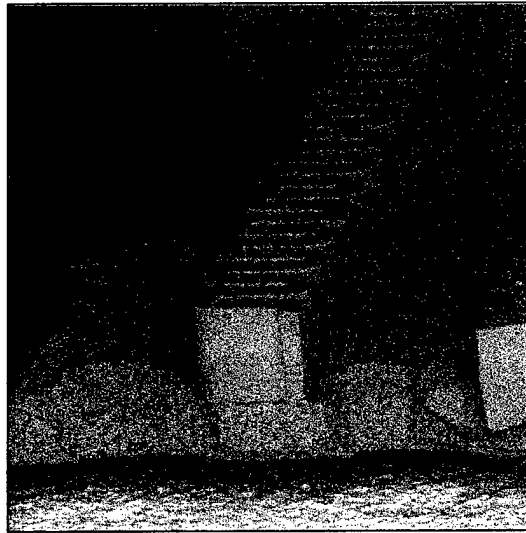
**Figure 19 SEM micrograph showing a 400 GHz folded waveguide TWT circuit mold (negative) fabricated in SU-8 photoresist using UV lithography. The serpentine wall height is approximately 250 microns and the width is approximately 50 microns. The "pitch" (distance between bends) is approximately 100 microns.**

Using the same 400 GHz optical mask, investigations have also been initiated to assess deep reactive ion etching (DRIE) of silicon as a third method to produce circuit molds. Three approaches are considered possible: (1) to etch the serpentine trenches into the silicon, coat the result with gold or copper and use the resulting structures as the TWT circuits, (2) to etch the serpentine trenches into the silicon, and use the resulting structure as a master form for polymer micromolding, (3) to etch around the serpentine shape, leaving a serpentine "wall". The latter approach would treat the silicon as sacrificial, similar to the role that the PMMA or SU-8 "negative image" molds play in LIGA. The second and third approaches are considered more appropriate for larger, millimeter wave TWT circuits below 200 GHz, where special, extra thick wafers will be needed. The first approach is considered a reasonable option for THz regime circuits above 300 GHz. Figure 20 shows both optical microscope and SEM images from a preliminary DRIE effort using the same available 400 GHz optical mask. Again, the results are promising, but more process development will be required to evaluate the technical feasibility of the approach.
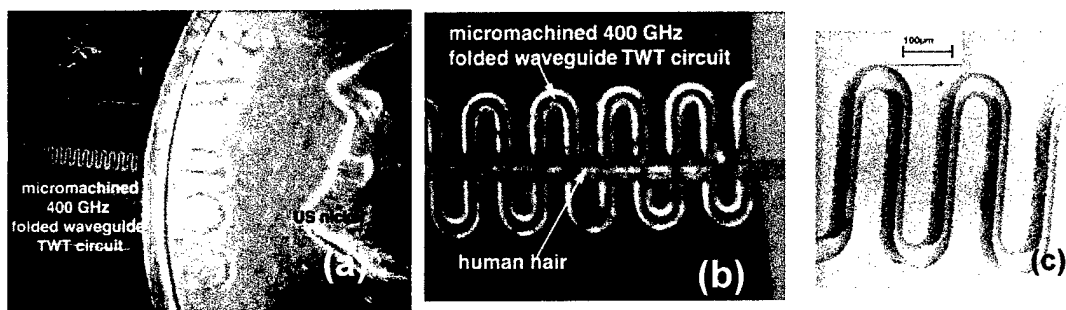
**Figure 20 Microfabrication of THz regime (400 GHz) folded waveguide TWT circuits using Deep Reactive Ion Etching (DRIE). A folded (serpentine) trench is etched in silicon with a DRIE tool, and then has been gold-plate for SEM imaging. (a) view of the miniature serpentine trench compared to US nickel. (b) close-up view compared to a 60 μm diameter human hair (c) SEM micrograph of the serpentine trench.**

The last microfabrication technique that has been explored is polymer micromolding. Polymer micromolding is a very recent addition to the MEMS scientist's toolbox, even though it has been anticipated for many years. The challenge has been to find suitable polymers and processing chemistries that can fill sub-millimeter features (often with large depth-to-width aspect ratios) with reliable reproduction of the original master. During the past few years, a candidate material has been identified, and some preliminary success by several researchers has been reported. That material is polydimethylsiloxane (PDMS), a silicone-type compound [14]. We have begun developing our own experience with this new material and microfabrication method. No serpentine or other waveguide structures have been fabricated yet. However, we have verified that the process is capable of replicating structures with features smaller than 10 μm. We have also determined that it is valuable to thin-film coat a mold with a teflon-like coating prior to pouring the PDMS into the mold to prevent adhesion after curing. There are facilities and expertise to do this coating at the University of Wisconsin. As of the completion date of this contract, a serpentine waveguide master mold is being fabricated. Upon completion, it will be teflon-coated and then used in micromolding experiments.

During the course of this project, a new, custom electron gun was designed, ordered, and built by Northrop Grumman Corporation (NGC—*note: in the original Phase II proposal, we included the purchase of a sheet beam thermionic electron gun. The estimate for the cost of the original sheet beam gun from Litton Electron Devices was $150,000. Since the proposal submission, NGC acquired Litton Electron Devices and the research objectives were modified so that an alternative gun was required*). The purpose of the NGC gun was to conduct experimental evaluations of micromachined folded waveguide TWTs. As of the completion of this contract, such tests still await the completion of microfabricated circuits, and will be conducted at a future date using alternative funding sources. The specifications for the NGC gun which cost approximately $50,000 are:

Beam voltage: 12 - 13 kV
Beam current: 90-110 mA
Beam radius: > or = 0.1 mm

Beam tunnel radius: > 0.3 mm

# 4 Personnel Supported

**Analex Corporation**
Carol Kory (co-PI) completed computational analyses using MAFIA and TWA3. Christine Chevalier investigated an alternative 3D EM code, Microwave Studio, to determine if it can be used to provide more accurate and computationally efficient cold-test data.

**University of Wisconsin – Madison**
John H. Booske (co-PI) conducted design calculations and completed computational analyses using CHRISTINE1D. Won-Je Lee simulated and evaluated waveguide circuit components (e.g., waveguide tapers and bends, aperture couplers) for the recirculated-feedback FWG-TWT oscillator using HFSS. Sean Gallagher researched the microfabrication techniques. Kamlesh Jain worked on experimental assembly and preliminary measurements for early tests of the oscillator concept using a scaled 40-55 GHz FWG-TWT on loan from Northrop Grumman Corporation. Sudeep Bhattacharjee carried out the experimental investigations. Booske has co-supervised the activities of Lee, Jain, Gallagher and Bhattacharjee in collaboration with faculty colleague Prof. Dan van der Weide.

# 5 Publications

S. Bhattacharjee, J.H. Booske, C.L. Kory, D.W. van der Weide, W.J. Lee, S. Limbach, M.R. Lopez, R.M. Gilgenbach, "A compact folded waveguide traveling wave tube oscillator for the generation of terahertz radiation: simulations and scaled experiments," to be submitted to *IEEE Trans. Microwave Thy & Tech* (in preparation, 2003).

C. L. Kory, J. H. Booske, W.-J. Lee, S. Gallagher, D. W. van der Weide, S. Limbach, and S. Bhattacharjee, THz radiation using high power, microfabricated, wideband TWTs, Proceedings of the 2002 IEEE MTT-S International Microwave Symposium, Seattle, WA, June 2-7, 2002.

S. Bhattacharjee, C. L. Kory, W. –J. Lee, S. Gallagher, D. W. van der Weide, J. H. Booske, S. Limbach, Comprehensive simulations of compact THz radiation sources using microfabricated, folded waveguide TWTs, Proceedings of the Third International Vacuum Electronics Conference (IVEC 2002), Monterey, California (April 23 – 25), pp. 26 – 27, 2002.

John H. Booske, New opportunities in Vacuum Electronics through application of microfabrication technologies, Proceedings of the Third International Vacuum Electronics Conference (IVEC 2002), Monterey, California (April 23 – 25), pp. 11 – 12, 2002.

J.H. Booske, D.W. van der Weide, C. L. Kory, S. Limbach, W. Lee, S. Gallagher and P. Gustafson, Micromachined TWTs for THz Radiation Sources, IEEE International Vacuum Electronics Conference (IVEC), Noordwijk Proceedings, The Netherlands, April 2-4, 2001.

J.H. Booske, C.L. Kory, D. Gallagher, V. Heinen, K. Kreischer, D.W. van der Weide, S. Limbach, P.J. Gustafson, W.-J. Lee, S.M. Gallagher, K. Jain, Terahertz-Regime, Micro-VEDs:

Evaluation of Micromachined TWT Conceptual Designs, IEEE Pulsed Power Plasma Science (PPPS)-2001 Conference Proceedings, Las Vegas, June 17-22, 2001.

M.C. Converse, S.C. Hagness, J.H. Booske, Y.Y. Lau[1], C.L. Kory[2], M.M. McNeely, M.A. Wirth, J.E. Scharer, C. Wilsen, Investigation of Ultrawideband Pulses in Wideband Helix Traveling Wave Tubes: Theory and Simulation, IEEE Pulsed Power Plasma Science (PPPS)-2001 Conference Proceedings, Las Vegas, June 17-22, 2001.

J.H. Booske, W.-J. Lee, S. Gallagher, D. van der Weide, and K. Jain, C.L. Kory, Microfabricated TWTs as high power, wideband sources of THz radiation, *9th International Conference on Terahertz Electronics*, Charlottesville, VA, 15-16 October, 2001.

# 6 Interactions/Transitions

**Presentations** were made at the following international, refereed conferences:

C. L. Kory, J. H. Booske, W.-J. Lee, S. Gallagher, D. W. van der Weide, S. Limbach, and S. Bhattacharjee, THz radiation using high power, microfabricated, wideband TWTs, 2002 IEEE MTT-S International Microwave Symposium, Seattle, WA, June 2-7, 2002.

S. Bhattacharjee, C. L. Kory, W. –J. Lee, S. Gallagher, D. W. van der Weide, J. H. Booske, S. Limbach, Comprehensive simulations of compact THz radiation sources using microfabricated, folded waveguide TWTs, Third International Vacuum Electronics Conference (IVEC 2002), Monterey, California (April 23 – 25), 2002.

John H. Booske, New opportunities in Vacuum Electronics through application of microfabrication technologies, Third International Vacuum Electronics Conference (IVEC 2002), Monterey, California (April 23 – 25), 2002.

J.H. Booske, D.W. van der Weide, C. L. Kory, S. Limbach, W. Lee, S. Gallagher and P. Gustafson, Micromachined TWTs for THz Radiation Sources, IEEE International Vacuum Electronics Conference (IVEC), Noordwijk, The Netherlands, April 2-4, 2001.

J.H. Booske, C.L. Kory, D. Gallagher, V. Heinen, K. Kreischer, D.W. van der Weide, S. Limbach, P.J. Gustafson, W.-J. Lee, S.M. Gallagher, K. Jain, Terahertz-Regime, Micro-VEDs: Evaluation of Micromachined TWT Conceptual Designs, IEEE Pulsed Power Plasma Science (PPPS)-2001, Las Vegas, June 17-22, 2001.

M.C. Converse, S.C. Hagness, J.H. Booske, Y.Y. Lau[1], C.L. Kory[2], M.M. McNeely, M.A. Wirth, J.E. Scharer, C. Wilsen, Investigation of Ultrawideband Pulses in Wideband Helix Traveling Wave Tubes: Theory and Simulation, IEEE Pulsed Power Plasma Science (PPPS)-2001, Las Vegas, June 17-22, 2001.

J.H. Booske, W.-J. Lee, S. Gallagher, D. van der Weide, and K. Jain, C.L. Kory, Microfabricated TWTs as high power, wideband sources of THz radiation, *9th International Conference on Terahertz Electronics*, Charlottesville, VA, 15-16 October, 2001.

S. Bhattacharjee, J. H. Booske, W. J. Lee, C. L. Kory, S. Gallagher, M. Genack, D. W. van der Weide, S. Limbach, M. R. Lopez, R. M. Gilgenbach, A compact folded waveguide traveling wave tube oscillator for the generation of terahertz radiation, 44th Annual Meeting of the Division of Plasma Physics (APSDPP), Orlando, Florida, November 11 - 15 (2002). [Bull. Am. Phys. Soc., **47**, 256 (2002)].

In the area of **transitions**, Northrop Grumman Electronic Systems sector (Vacuum Electronics Research, Development, and Engineering) has already adopted our idea of micro-fabrication of folded waveguide circuits for advanced FWG-TWT production. In particular, they are investigating LIGA-fabricated FWG-TWTs for advanced, lower cost, high yield mm-wave (~ 100 GHz) slow-wave amplifiers. The enabling research was the conceptualization of how to adopt micro-fabrication techniques (such as those critical to the realization of THz TWTs) to the manufacture of precision, high frequency, folded waveguide circuits for lower cost, higher yield, mm-wave and THz regime TWTs. Likewise, Calabazas Creek Research has also adopted this idea as the basis for investigating development of mmwave (40 – 200 GHz) TWTs for DoD satellite communications applications.

# 7 New Discoveries

Invented and completed feasibility analyses for micro-fabricated TWTs that will enable low-cost, extremely-high-data-rate (> 10 GB/s) advanced digital communications capabilities using THz frequencies, as well as lower cost, higher yield production of millimeter-wave slow-wave amplifiers for air-borne radar and missile seeker technologies.

# 8 Honors/Awards

Plenary talk: J. H. Booske, "New opportunities in vacuum electronics through the application of microfabrication technologies", IVEC 2002, Monterey, California.

# 9 References

1 G. Caryotakis, G. Scheitrum, et al., The klystrino: a high power W-band amplifier, *International Vacuum Electronics Conference 2000* (Monterey, CA, USA, 2-4 May, 2000), paper 1.5.
2 J. W. Digby, et al, 2000, Fabrication and Characterization of Micromachined Rectangular Waveguide Components for Use at Millimeter-Wave and Terahertz Frequencies, IEEE Trans. MTT, 48, 8, 1293-1302.
3 K. Takahata and Y. Gianchandani, 2001, Batch mode micro-EDM for high-density and high-throughput micromachining, IEEE International Conference on Micro Electro Mechanical Systems, Interlochen, January.
4 See for example, http://www.stssystems.com.
5 NATO Advanced Research Workshop, "Terahertz Sources and Systems," (Chateau de Bonas, Gascony, France, 22-28 June, 2000).

6  P.H. Siegel, H. Manohara, J. Xu, B. Chang, A. Husain, and J. Hone, "Design and Fabrication of a 1200 GHz Nanoklystron," Proceedings of the 9th Int. Conf. On THz Electronics (Charlottesville, VA, Oct 15-16, 2001).

7  J. East and G. Haddad, "Vacuum Based Sources for THz Applications," Proceedings of the 9th Int. Conf. On THz Electronics (Charlottesville, VA, Oct 15-16, 2001).

8  J.H. Booske and D.W. van der Weide, 2000, Ultraminiature terahertz traveling wave tubes made by micromachining, Patent Disclosure P01086US, University of Wisconsin.

9  G. Dohler, D. Gallagher, and J. Richards, 1993, Millimeter wave folded waveguide TWTs, Vacuum Electronics Annual Review Proceedings (Crystal City, VA), pp. V15-V20.

10  T. Weiland, 1985, On the Unique Numerical Solution of Maxwellian Eigenvalue Problems in Three Dimensions, Part. Accel., vol. 17, pp. 227-242.

11  Ansoft HFSS: 3D EM simulation software for RF, Wireless, Packaging, and Opto-electronic design (http://www.ansoft.com/products/hf/hfss/index.cfm)

12  D.M. MacGregor, 1993, Two-dimensional nonlinear multisignal helix traveling-wave tube amplifier computer program, Volume 1: User Manual, Electrocon International, Inc., Ann Arbor, MI, USA.

13  T.M. Antonsen, Jr. and B. Levush, 1998, Traveling-wave tube devices with nonlinear dielectric elements, IEEE Trans. Plasma Sci., 26, 775-786.

14  S.W. Park, K.S. Kim, W.A. Davis, and J.B. Lee, "Wafer Level Batch Transfer Process of RF MEMS Passive Device Using PDMS," International Microelectronics and Packaging Society Meeting 2002, Sept 3-6, 2002, Denver CO.